Susceptibility quantification in MRI using phase gradient mapping

L. Wang[1], and Q. Zhao[1]
[1]Department of Physics and Astronomy, University of Georgia, Athens, GA, United States

Introduction: Susceptibility quantification in MRI is a novel technique that can be involved in many applications, such as tracking stem cells labeled with super-paramagnetic iron oxide (SPIO) nanoparticles. Because of the tight relationship between susceptibility and magnetic field inhomogeneity, most of the published techniques employ the MR phase images to estimate susceptibility distributions. However, the wrapping effect in MR phase maps is a headachy problem and has to be solved before any further data processing. In this work, we present a new technique that implements the phase gradient mapping (PGM) method to directly calculate the susceptibility distribution.

Theory and Methods: In the MR images acquired by using gradient echo sequences, magnetic field inhomogeneity is connected with the phase maps according to the relationship $\Delta B = -\varphi/\gamma T_E$. The gradients of the magnetic field inhomogeneity can then be correctly derived by taking the gradients of the phase maps, since the wrapping problem associated with the phase maps will be solved by the PGM methods [1,2]. Theoretical studies demonstrate that in the k-space, the Fourier transform of the normalized magnetic field inhomogeneity is equal to a point-wise multiplication of the Fourier transform of the susceptibility distribution and the Fourier transform of a magnetic dipole, given by $(1/3-k_z^2/k^2)$ [3]. This allows the susceptibility to be calculated by solving the inverse problem, which is formulated as $\chi = F^{-1}(F(\Delta B/B_0)(1/3-k_z^2/k^2)^{-1})$, where F and F^{-1} mean the forward and inverse Fourier transform, respectively. However, this is a notorious ill-posed inverse problem since the elements of the term $(1/3-k_z^2/k^2)$ along the magic angles are equal to zero. The Tikhonov regularization technique is a powerful tool to make such an inverse problem better conditioned by adding spatial information extracted from MR magnitude maps [4]. Thus, based on the combination of the PGM method and Tikhonov regularization technique, we proposed that the susceptibility estimation can be reached by solving the following two gradient-based least square problems:

$$\min_\chi \sum_{i=1}^{3}\left\| W_{x_i}(F^{-1}i2\pi k_i DF\chi - \frac{\partial}{\partial x_i}\delta_B)\right\|_2^2 + \alpha^2\|W_0\chi\|_2^2 + \beta^2\sum_{i=1}^{3}\left\|W_{1x_i}F^{-1}i2\pi k_i F\chi\right\|_2^2 \quad (1),$$

$$\text{or } \min_\chi \sum_{i=1}^{3}\left\| W_{x_i}(G_{x_i}F^{-1}DF\chi - \frac{\partial}{\partial x_i}\delta_B)\right\|_2^2 + \alpha^2\|W_0\chi\|_2^2 + \beta^2\sum_{i=1}^{3}\left\|W_{1x_i}G_{x_i}\chi\right\|_2^2 \quad (2)$$

where δ_B represents the normalized magnetic field inhomogeneity $\Delta B/B_0$, W_x is a weighting matrix containing the inverse of the standard deviation of the PGM. W_0 is a mask whose elements are equal to zero or one when they are inside or outside of the region-of-interest. W_{1x} is another weighting matrix containing the inverse of the gradients of the MR magnitude map. α and β are two different regularization parameters.

The difference between the two methods is that in formula (1), gradients are calculated based on the derivative property of the Fourier transform, while in formula (2), gradients are calculated by multiplying a gradient matrix G_x, which is derived from the central difference formula. The gradients of δ_B along x-, y- or z-direction can be all involved or selectively involved to calculate susceptibility distributions.

To validate the proposed susceptometry techniques, a 2% agar phantom with two embedded cylindrical, plastic vials containing different concentrations of SPIO nanoparticles (10 nm Fe_3O_4 nanocrystals, NN Labs, Fayetteville, AR) was constructed. The concentrations of SPIO nanoparticles were 300 μg/mL and 200 μg/mL in the vial 1 and vial 2, respectively (see Fig 1a.). The vial diameter was 1.2 cm, the wall thickness of the vial was 1 mm, and the volume of the vial was 5 mL. Experiments were performed using a 3-T clinical MRI system (GE Healthcare, Waukesha, WI). The phantom was standing vertically on the patient table, perpendicular to the main magnetic field B_0. A standard birdcage radio-frequency coil was used for data acquisition with a three-dimensional gradient echo pulse sequences. The scan parameters were: TE_1 = 5 ms, TE_2 = 7 ms, TR = 250 ms, flip angle = 60 degrees, FOV = 11 cm, slab thickness of the sample = 4.2 cm, 128 × 128 acquisition matrix, 28 coronal slices, radio-frequency bandwidth = 15.6 kHz.

In order to compare the results obtained from the two different formulas and find the optimal choice of β, the conjugate gradient least square algorithm [5] was utilized as the inverse problem solver with the regularization parameter β ranged from 10^{-3} to 10^3. Furthermore, to test the stability of the techniques on different noise levels, additional Gaussian noise was added into the original phantom dataset to generate a dataset with lower SNR. The data processing was coded and realized using Matlab (the Mathworks inc, Massachusetts).

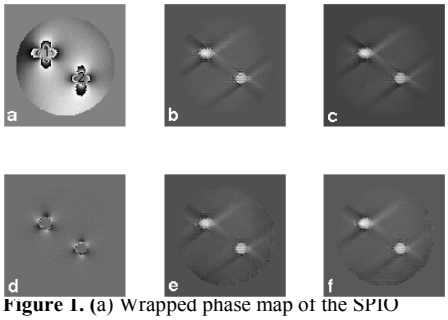

Figure 1. (a) Wrapped phase map of the SPIO phantom. (d) Gradient map of δ_B field along x-direction. Susceptibility distributions estimated in different conditions: (b) SNR=90, using formula (1), (c) SNR=90, using formula (2), (e) SNR=30, using formula (1), and (f) SNR=30, using formula (2).

Results and Discussion: Fig. 1(d) illustrated the x-gradient of δ_B extracted from the phase map (see Fig. 1(a)), where the influence of the phase wrapping effect had been eliminated. Fig. 1 (b), (c), (e) and (f) illustrated the estimated susceptibility distributions. As expected, Fig. 1 (e) and (f) (with a low SNR of 30) appeared more noisy than (b) and (c) (with a high SNR of 90). Furthermore, we can see obvious cross-shaped artifacts in the four images, since the ill-posed condition of the inverse problem cannot be totally eliminated by the Tikhonov regularization technique.

Fig. 2 showed the results of susceptibility estimate and corresponding standard deviations as s function of β under the low SNR condition. All of the four sub-figures suggested that the optimized results were achieved when β was around 10^{-1}, as the estimated susceptibilities kept stable instead of seriously decay while β was increasing, until β became larger than 10^{-1}, at the meantime, the standard deviations reached the lowest points compared with other stable results.

Table 1 listed the results of the phantom datasets derived using the proposed two different methods with both high and low SNRs, when β was equal to 10^{-1}. As seen in the table, the method (1) results in an estimate of smaller susceptibility compared with that of the method (2), consistent with the results shown in Fig. 2. Also, a lower SNR results in estimate of smaller susceptibilities. The estimated susceptibilities were finally converted into molar susceptibility of Fe_3O_4 nanocrystals. Compared with the literature value of molar susceptibility of Fe^{3+} in Ferridex (3733 L/mol) at 3 T [6], the Fe^{3+} in the Fe_3O_4 nanocrystals generates about the similar amount of magnetization.

	Vial1 (ppm)	Vial2 (ppm)	χ_{mol} (L/mol)
SNR=90, F(1)	4.28±0.91	3.16±0.86	3481±883
SNR=90, F(2)	4.93±0.79	3.62±0.67	3995±725
SNR=30, F(1)	3.90±0.66	2.96±0.64	3218±668
SNR=30, F(2)	4.54±0.71	3.46±0.68	3751±727

Table 1. Estimated susceptibilities of the two vials and molar susceptibility of the Fe_3O_4 nanocrystals with different formulas and noise levels, when log(β) is equal to -1.

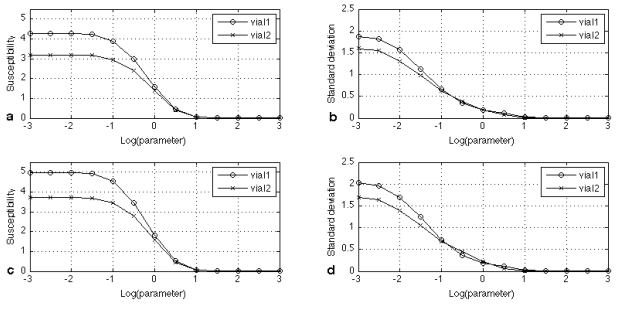

Figure 2. Plots of the estimated susceptibilities (left panel)and their corresponding standard deviations (right panel) vs. the logarithms of different parameters β for the phantom data with SNR of 30.

Conclusion: The proposed gradient-based techniques enable a fairly accurate estimation of susceptibility under different noise levels from the phase gradient maps, without requiring any phase unwrapping process.

References: [1] Bakker, et al, Phys Med Biol, 53(2008). [2] Zhao, et al. NMR Biomed, 2010 [3] Deville, et al, Concepts Mag Reson, 19(2003). [4] Rochefort, et al, MRM, 63(2010). [5] Hestenes, et al, J Res Natl Bureau Standards, 49(1952). [6] Rochefort, et al, MRM, 60(2008).